In vivo, label-free, three-dimensional quantitative imaging of liver surface using multi-photon microscopy

Citation: Zhuo, Shuangmu, Jie Yan, Yuzhan Kang, Shuoyu Xu, Qiwen Peng, Peter T. C. So, and Hanry Yu. "In Vivo, Label-Free, Three-Dimensional Quantitative Imaging of Liver Surface Using Multi-Photon Microscopy." Applied Physics Letters 105, no. 2 (July 14, 2014): 023701. © 2014 AIP Publishing LLC

As Published: http://dx.doi.org/10.1063/1.4890593

Publisher: AIP Publishing

Persistent URL: http://hdl.handle.net/1721.1/120483

Version: Final published version: final published article, as it appeared in a journal, conference proceedings, or other formally published context

In vivo, label-free, three-dimensional quantitative imaging of liver surface using multi-photon microscopy

Shuangmu Zhuo,[1,2,a),b)] Jie Yan,[1,3,4,b)] Yuzhan Kang,[1] Shuoyu Xu,[1,3,5] Qiwen Peng,[3,5,6] Peter T. C. So,[1,5,7,8] and Hanry Yu[1,3,4–6,8,a)]

[1]*Biosystems and Micromechanics IRG, Singapore-MIT Alliance for Research and Technology, 1 CREATE Way, #04-13/14 Enterprise Wing, 138602 Singapore*
[2]*Institute of Laser and Optoelectronics Technology, Fujian Normal University, Fuzhou 350007, China*
[3]*Institute of Bioengineering and Nanotechnology, 31 Biopolis Way, #04-01, 138669 Singapore*
[4]*Department of Physiology, Yong Loo Lin School of Medicine, National University of Singapore, 14 Medical Drive, MD 11 #04-01A, 117599 Singapore*
[5]*Computation and System Biology Program, Singapore-MIT Alliance, 4 Engineering Drive 3, E4-04-10, 117576 Singapore*
[6]*Mechanobiology Institute, 5A Engineering Drive 1, T-Lab #05-01, 117411 Singapore*
[7]*Department of Mechanical Engineering, Massachusetts Institute of Technology, 77 Massachusetts Avenue, Cambridge, Massachusetts 02139, USA*
[8]*Division of Biological Engineering, Massachusetts Institute of Technology, 77 Massachusetts Avenue, Cambridge, Massachusetts 02139, USA*

(Received 23 April 2014; accepted 7 July 2014; published online 16 July 2014)

Various structural features on the liver surface reflect functional changes in the liver. The visualization of these surface features with molecular specificity is of particular relevance to understanding the physiology and diseases of the liver. Using multi-photon microscopy (MPM), we have developed a label-free, three-dimensional quantitative and sensitive method to visualize various structural features of liver surface in living rat. MPM could quantitatively image the microstructural features of liver surface with respect to the sinuosity of collagen fiber, the elastic fiber structure, the ratio between elastin and collagen, collagen content, and the metabolic state of the hepatocytes that are correlative with the pathophysiologically induced changes in the regions of interest. This study highlights the potential of this technique as a useful tool for pathophysiological studies and possible diagnosis of the liver diseases with further development. [http://dx.doi.org/10.1063/1.4890593]

Dynamic structural features on the liver surface can reflect functionally significant changes in the liver.[1–3] For the physiological studies and disease diagnosis of the liver, the ability to visualize the different structural features of the liver surface with micrometer-scale resolution under *in vivo* conditions would provide a major step forward. Although several methodologies to probe liver have been developed in the last decades,[4,5] the major limitation remains the absence of label-free and high-resolution methods that provide a fast quantitative visualization of various surface features in the native microenvironment of the living tissue.

A promising method for obtaining detailed structural and functional information on the liver surface at subcellular and cellular level is multi-photon microscopy (MPM).[6–9] MPM relies on the nonlinear excitation of fluorescent molecules or the induction of second harmonic generation: two near-infrared wavelength photons interact simultaneously with a molecule or structure, resulting in the emission of one visible range photon (Fig. 1(a)). Since signal generation in MPM occurs in a confined volume, it has the three dimensional subcellular spatial resolution. Specifically, by using the same excitation wavelength but separate detectors to visualize several intrinsic sources of contrast,[10–12] autofluorescence and second harmonic images can be obtained. This multimodal capability provides structural and functional information on unstained tissues with some levels of molecular specificity that is not accessible using other noninvasive methods. Previous studies have shown the use of two-photon excited fluorescence (TPEF) for visualizing the distribution of intrinsic molecules such as reduced pyridine nucleotide (NAD(P)H), oxidized flavoproteins (Fp), elastin, and others.[10–13] Second-harmonic generation (SHG) has been proven to be a sensitive probe of the structural organization of collagen in tissues[14–17] and is therefore an effective approach for imaging collagen fibers in the liver.[3,18]

There has been no report on efforts to exploit MPM for *in vivo*, label-free, three-dimensional quantitative imaging of liver surface. Here, we aimed to demonstrate the feasibility of using MPM to visualize various structural features of liver surface in living rats and quantitatively compare changes in a well-established disease model.[19]

Multiphoton imaging was achieved using a nonlinear optical system described previously,[3] as shown in Fig. 1(b). In brief, multi-photon images were acquired using a commercial laser scanning microscopic imaging system (Zeiss LSM 510 META, Jena, Germany) coupled to a femtosecond Ti: sapphire laser (Mai-Tai broadband, Spectra-Physics) operating at 810 nm. The polarization direction of the laser

a)Authors to whom correspondence should be addressed. Electronic addresses: shuangmuzhuo@gmail.com and hanry_yu@nuhs.edu.sg.
b)S. Zhuo and J. Yan contributed equally to this work.

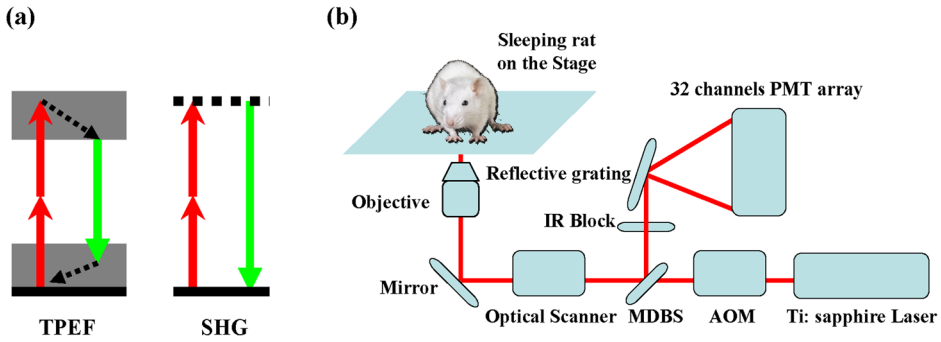

FIG. 1. (a) Principle of the TPEF/SHG. (b) Schematic of the experimental setup.

light is the horizontal polarization. An oil immersion objective (×40 and NA = 1.3) was employed for focusing the excitation beam into tissue samples (average power less than 10 mW) and was also used to detect the intrinsic TPEF and SHG signals. This system has eight channels, which can selectively be set to detect emission signals within the range from 377 to 716 nm to achieve imaging. In this work, three channels were used: two channels (430–490 nm and 500–560 nm) were used to collect TPEF signals, whereas another channel (390–410 nm) was used to record SHG signal. These three channels possessed the same system parameters, including laser power, detector gain, amplifier gain, and amplifier offset. Collagen belongs to noncentrosymmetric molecules and is an efficient sources of SHG,[14,15] so the SHG (390–410 nm) signal results from collagen, primarily types I and III, the major fibrous collagen.[3,18] According to the previous studies and liver structure,[1,3,6,9,20,21] the capsular TPEF (430–490 nm and 500–560 nm) mainly results from the elastin, whereas the sub-capsular TPEF (430–490 nm) signal originates from NAD(P)H and the sub-capsular TPEF (500–560 nm) signal mainly arises from Fp. Moreover, the ratio of NAD(P)H over Fp fluorescence, called the redox ratio, is a good indicator of the cellular metabolic state.[12,19,20] The images were obtained at 2.56 μs per pixel. To change and record the focus position, a fine focusing stage (HRZ 200 stage, Carl Zeiss) was used.

A total of six Male Wistar rats weighing 200–300 g were used with the approval of the Institutional Animal Care and Use Committee. Common bile duct ligation (BDL) was performed as described previously as a well-established disease model for biliary atresia, the major cause of infant death,[19] and animals were studied 5 weeks after surgery. Three normal control animals and three animals that underwent BDL were studied. For *in vivo* imaging, rats were anesthetized using ketamine (75 mg/kg) and xylazine (10 mg/kg). A midline incision of abdomen skin and muscle was created after shaving. After prone positioning of the rat, the liver was gently withdrawn from the abdominal cavity and placed over a glass coverslip on the stage of a Zeiss Axiovert 200 microscope. Multi-photon images were recorded from the capsular and sub-capsular regions of liver surface. Each rat preparation and *in vivo* imaging was completed within 2 h.

Shown in Figs. 2 and 3 are the representative multi-photon images from *in vivo* normal and abnormal (BDL) rat livers at different depths (capsular and sub-capsular regions). For the purpose of distinguishing the SHG and TPEF signals, pseudocolors of grey (SHG: 390–410 nm), green (TPEF: 430–490 nm), and red (TPEF: 500–560 nm) were assigned. It

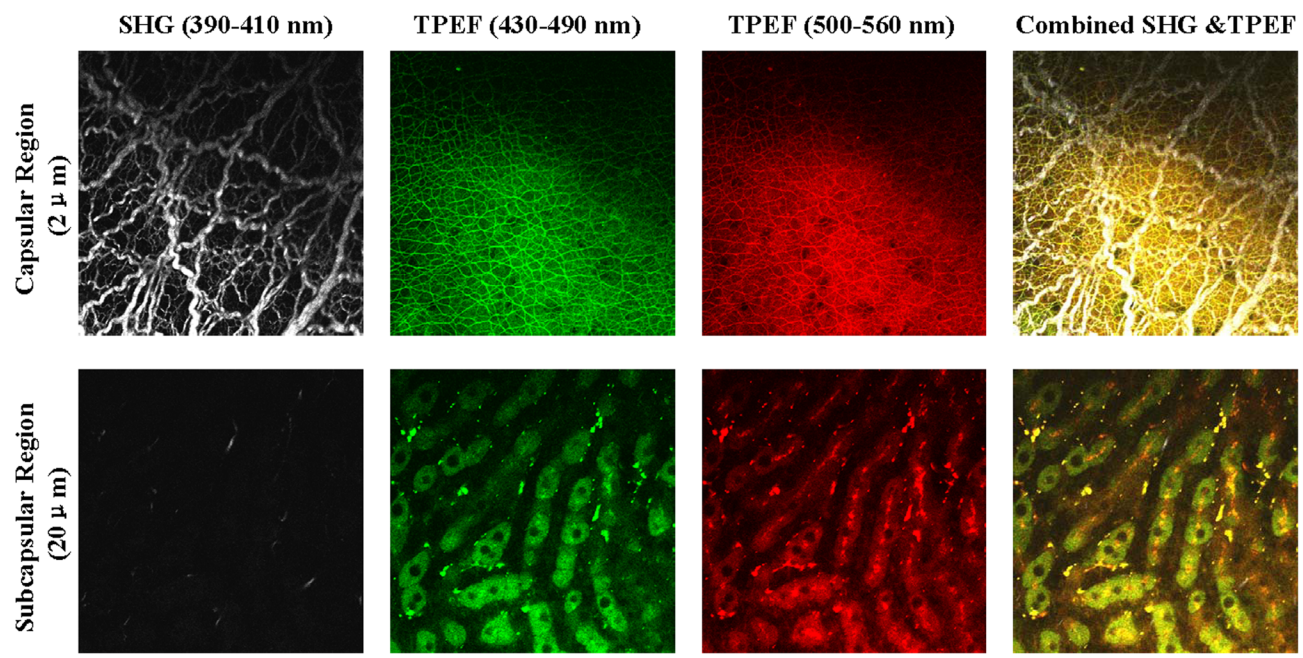

FIG. 2. Representative multi-photon images acquired from *in vivo* normal rat liver. From left to right: SHG, TPEF, and combined SHG and TPEF images. Top to bottom: capsular region and sub-capsular region. The excitation wavelength λ_{ex} was 810 nm. The size of images is 225 × 225 μm^2.

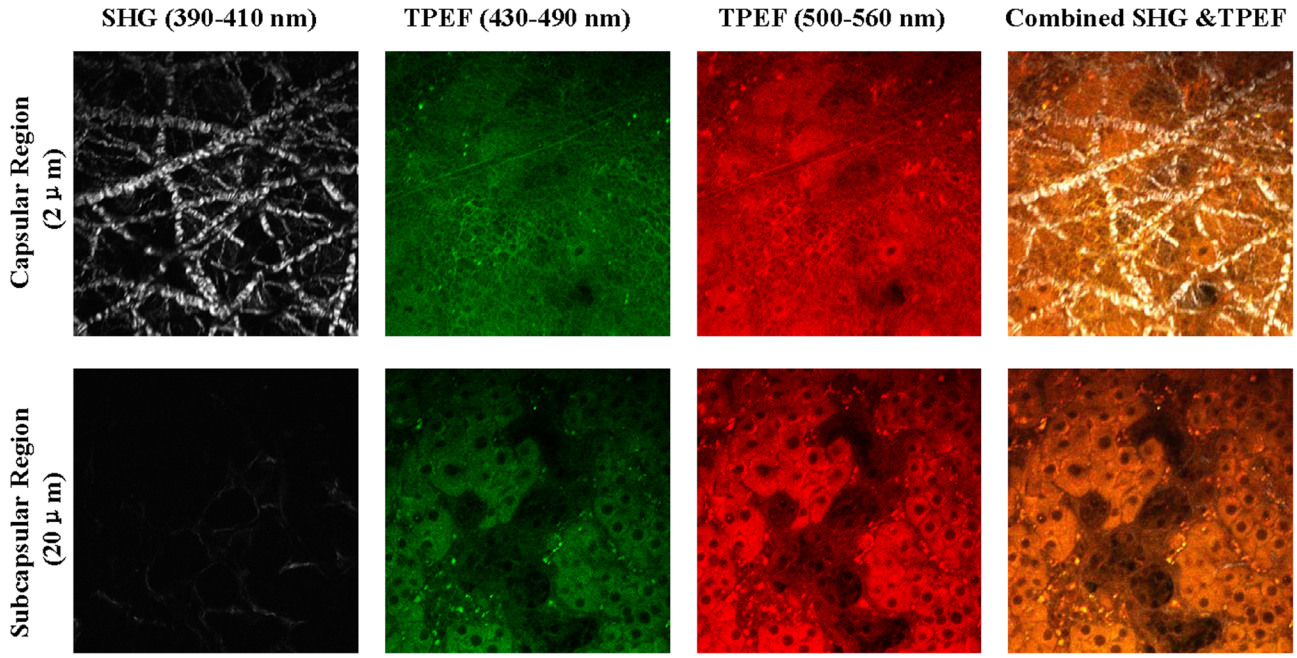

FIG. 3. Representative multi-photon images acquired from *in vivo* abnormal rat liver. From left to right: SHG, TPEF, and combined SHG and TPEF images. Top to bottom: capsular region and sub-capsular region. The excitation wavelength λ_{ex} was 810 nm. The size of images is $225 \times 225\ \mu m^2$.

is seen in Figs. 2 and 3 that several interesting results are obtained. First, in the normal capsular region collagen is dense with curry sub-filament structures and elastin displays a fine structure with visible fibers, whereas in the abnormal capsular region collagen is less dense and straight with loss of curry sub-filament structures and elastin shows a breakage of fine structure with merged fibers. Second, in comparison with the normal capsular region, the abnormal capsular region has an alteration in the proportions between collagen and elastin, as shown in the combined SHG&TPEF figures. Third, in the normal sub-capsular region there are well-organized hepatocytes and only a little collagen is presented; whereas in the abnormal sub-capsular region there are some hepato-necrotic areas because of bile duct cell proliferation and some abnormal collagen, a clear indication of fibrosis, is also presented. Last, in the sub-capsular region, the abnormal hepatocytes display a light yellow, whereas the normal hepatocytes exhibit a more green color, as seen in the combined SHG&TPEF figures. Since green and red combines to yield yellow color, a light yellow indicates that the proportion of Fp signals (red) increases in abnormal case, while a more green reflects that the proportion of NAD(P)H signals (green) increases in normal case. In other words, the abnormal hepatocytes show a lower redox ratio, whereas the normal hepatocytes display a higher redox ratio.

To further quantify these changes on liver surface, we performed quantitative analyses on the images from the capsular and sub-capsular layers. We randomly selected five 225 μm by 225 μm rectangular areas per layer per rat for quantitative analysis. For the capsule, three analyses were performed. First, we measured the sinuosity of collagen fiber (SCF). In each rectangular area, the curvilinear length (along the fiber) is defined as a, and the distance (straight line) between the end points of the fiber is defined as b. The sinuosity of collagen fiber is defined as a/b. It was found that the SCF of normal rats is significantly higher than that of abnormal rats. To be specific, the SCF in normal rats is 1.50 ± 0.13 and in abnormal rats it is 1.26 ± 0.06. This observation supports the notion that BDL leads to higher expansion force on the liver surface, which causes straight collagen fibers. Second, the elastic fiber structure (EFS) was analyzed by using the gray-level co-occurrence matrix (GLCM) texture module of ImageJ software (NIH), as reported previously.[16,22] The GLCM can provide texture features based on gray-level statistical patterns between neighboring pixels. In particular, the correlation feature, a measure of intensity correlation as a function of pixel distance, relates to elastic fiber structure by indicating fiber and separation. Similar to the previous work,[15] the correlation value at the distance of 30 pixels is defined as the EFS. In this definition, a loss of fine structure leads to a big EFS. The EFS in normal rats is 0.26 ± 0.07, whereas in abnormal rats it is 0.59 ± 0.10, suggesting the loss of the fine elastic fibril structure in BDL rats. Third, we analyzed the ratio between elastin and collagen (REC). Since the average SHG signal can reflect the total collagen content (CC) and TPEF signals can represent the amount of elastin,[11,17,23] we performed the analysis of the ratio of SHG (390–410 nm) signal and TPEF (430–560 nm) signal. We found that the REC in normal rats is 1.72 ± 0.17, whereas in abnormal rats it is 2.51 ± 0.23, suggesting increased amount of elastin in BDL rats. This result also confirms the fact that there is the regulation of elastin secretion and turnover after BDL.[24]

For the sub-capsule, we performed two analyses. First, the CC was determined by counting the ratio of the SHG pixels over the whole pixels. In this definition, collagen increase results in a large collagen content value. The CC in normal rats is 0.005 ± 0.001 and in abnormal rats it is 0.023 ± 0.006, reflecting collagen increase in BDL rats. Second, the redox ratio (RR) in hepatocytes was calculated. The intensity of NAD(P)H spectral band (430–490 nm) and the intensity of Fp spectral band (500–560 nm) were defined as a and b,

TABLE I. Quantitative characterization parameters derived from multi-photon imaging.

	Capsular region			Subcapsular region	
	The sinuosity of collagen fiber (SCF)	Elastic fiber structure (EFS)	The ratio between elastin and collagen (REC)	Collagen content (CC)	The redox ratio of the hepatocytes (RR)
Normal liver	1.50 ± 0.13	0.26 ± 0.07	1.72 ± 0.17	0.005 ± 0.001	1.24 ± 0.12
Abnormal liver	1.26 ± 0.06	0.59 ± 0.10	2.51 ± 0.23	0.023 ± 0.006	0.38 ± 0.05

respectively. Then the redox ratio was calculated by using the following formula: a/b. We selected regions where the cells can be identified and performed the redox ratio analysis. For the abnormal rats, a significant decrease in the RR is observed. Quantitatively, the RR in normal rats is 1.24 ± 0.12, and in abnormal rats it is 0.38 ± 0.05. This observation supports the notion that there is a decrease in metabolic activity in BDL rats due to apoptosis of hepatocytes.[25]

Presented in Table I are the results of SCF, EFS, REC, CC, and RR from *in vivo* normal and abnormal rat livers. As Table I shows the SCF, EFS, REC, CC, and RR are significantly different between the normal and abnormal rat livers. From above results, one sees that these feature parameters derived from label-free multi-photon imaging are effective quantitative parameters for comparing pathophysiologically induced changes.

In summary, we have reported a label-free, three-dimensional quantitative and sensitive method for visualizing various structural features of liver surface in living rat with some levels of molecular specificity by the use of MPM. The ability of this method to label-freely extract quantitative biomorphologic and biochemical features *in vivo*, including the sinuosity of collagen fiber, the elastic fiber structure, the ratio between elastin and collagen, collagen content, and the metabolic state of the hepatocytes could provide a potential method for researchers or clinicians to compare pathophysiologically induced changes to aid pathology and non-invasive radiology investigation. With additional development,[26–28] this method has potential to become a useful tool for the pathophysiological studies and diagnosis of the liver diseases in the future.

This project was supported by the National Research Foundation Singapore, through the Singapore MIT Alliance for Research and Technology (SMART) Centre's BioSyM IRG research program. This project also is supported in part by the Institute of Bioengineering and Nanotechnology, Biomedical Research Council, A*STAR; grants from Janssen (R-185-000-182-592 and R-185-000-228-592), Singapore-MIT Alliance Computational and Systems Biology Flagship Project funding (C-382-641-001-091), SMART BioSyM and Mechanobiology Institute of Singapore (R-714-001-003-271) funding to H.Y. and the National Natural Science Foundation of China (61275006) and the Natural Science Foundation for Distinguished Young Scholars of Fujian Province (2014J06016) funding to S.Z.

[1]L. S. Friedman and E. B. Keeffe, *Handbook of Liver Disease*, 3rd ed. (Elsevier Saunders, Philadelphia, PA, 2011), pp. 19103–2899.
[2]A. Di Lelio, C. Cestari, A. Lomazzi, and L. Beretta, Radiology **172**, 389–392 (1989).
[3]Y. He, C. H. Kang, S. Xu, X. Tuo, S. Trasti, D. C. Tai, A. M. Raja, Q. Peng, P. T. So, J. C. Rajapakse, R. Welsch, and H. Yu, J. Biomed. Opt. **15**, 056007 (2010).
[4]R. Weissleder and M. J. Pittet, Nature **452**, 580–589 (2008).
[5]M. Goetz and R. Kiesslich, Am. J. Physiol. Gastrointest. Liver Physiol. **298**, G797 (2010).
[6]W. R. Zipfel, R. M. Williams, and W. W. Webb, Nat. Biotechnol. **21**, 1369–1377 (2003).
[7]T. L. Sun, Y. Liu, M. C. Sung, H. C. Chen, C. H. Yang, V. Hovhannisyan, W. C. Lin, W. L. Chen, L. L. Chiou, G. T. Huang, K. H. Kim, P. T. C. So, H. S. Lee, and C. Y. Dong, Appl. Phys. Lett. **95**, 193703 (2009).
[8]C. C. Wang, F. C. Li, W. C. Lin, Y. F. Chen, S. J. Chen, S. J. Lin, and C. Y. Dong, Appl. Phys. Lett. **97**, 113702 (2010).
[9]P. T. C. So, C. Y. Dong, and R. M. Barry, Annu. Rev. Biomed. Eng. **2**, 399–429 (2000).
[10]W. R. Zipfel, R. M. Williams, R. Christie, A. Y. Nikitin, B. T. Hyman, and W. W. Webb, Proc. Natl. Acad. Sci. U. S. A. **100**, 7075–7080 (2003).
[11]S. M. Zhuo, J. X. Chen, T. S. Luo, D. S. Zou, and J. J. Zhao, Opt. Express **14**, 7810–7820 (2006).
[12]J. N. Rogart, J. Nagata, C. S. Loeser, R. D. Roorda, H. Aslanian, M. E. Robert, W. R. Zipfel, and M. H. Nathanson, Clin. Gastroenterol. Hepatol. **6**, 95–101 (2008).
[13]S. M. Zhuo, J. Yan, G. Chen, J. X. Chen, Y. C. Liu, J. P. Lu, X. Q. Zhu, X. S. Jiang, and S. S. Xie, Biomed. Opt. Express **2**, 615–619 (2011).
[14]V. A. Hovhannisyan, P. J. Su, and C. Y. Dong, Appl. Phys. Lett. **94**, 233902 (2009).
[15]P. J. Campagnola and L. M. Loew, Nat. Biotechnol. **21**, 1356–1360 (2003).
[16]S. M. Zhuo, J. X. Chen, G. Z. Wu, S. S. Xie, L. Q. Zheng, X. S. Jiang, and X. Q. Zhu, Appl. Phys. Lett. **96**, 213704 (2010).
[17]E. Brown, T. McKee, E. diTomaso, A. Pluen, B. Seed, Y. Boucher, and R. K. Jain, Nat. Med. **9**, 796–800 (2003).
[18]L. Gailhouste, Y. Le Grand, C. Odin, D. Guyader, B. Turlin, F. Ezan, Y. Désille, T. Guilbert, A. Bessard, C. Frémin, N. Theret, and G. Baffet, J. Hepatol. **52**, 398–406 (2010).
[19]J. S. Gujral, A. Farhood, M. L. Bajt, and H. Jaeschke, Hepatology **38**, 355–363 (2003).
[20]M. C. Skala, K. M. Riching, A. Gendron-Fitzpatrick, J. Eickhoff, K. W. Eliceiri, J. G. White, and N. Ramanujam, Proc. Natl. Acad. Sci. U. S. A. **104**, 19494–19499 (2007).
[21]S. M. Zhuo, L. Q. Zheng, J. X. Chen, S. S. Xie, X. Q. Zhu, and X. S. Jiang, Appl. Phys. Lett. **97**, 173701 (2010).
[22]N. D. Kirkpatrick, J. B. Hoying, S. K. Botting, J. A. Weiss, and U. Utzinger, J. Biomed. Opt. **11**, 054021 (2006).
[23]S. J. Lin, S. H. Jee, C. J. Kuo, R. J. Wu, W. C. Lin, J. S. Chen, Y. H. Liao, C. J. Hsu, T. F. Tsai, Y. F. Chen, and C. Y. Dong, Opt. Lett. **31**, 2756–2758 (2006).
[24]C. Guyot, C. Combe, and A. Desmoulière, Histochem. Cell Biol. **126**, 517–523 (2006).
[25]H. Miyoshi, C. Rust, P. J. Roberts, L. J. Burgart, and G. J. Gores, Gastroenterology **117**, 669–677 (1999).
[26]M. Gu, H. C. Bao, and J. L. Li, J. Biomed. Opt. **15**, 050502 (2010).
[27]D. R. Rivera, C. M. Brown, D. G. Ouzounov, I. Pavlova, D. Kobat, W. W. Webb, and C. Xu, Proc. Natl. Acad. Sci. U. S. A. **108**, 17598–17603 (2011).
[28]K. König, A. Ehlers, I. Riemann, S. Schenkl, R. Bückle, and M. Kaatz, Microsc. Res. Tech. **70**, 398–402 (2007).